Chemical Physics 426 (2013) 16–22

Contents lists available at ScienceDirect

Chemical Physics

journal homepage: www.elsevier.com/locate/chemphys

Polarization-enhanced bonding process of halogen bond, a theoretical study on F–H/F–X (X = F, Cl, Br, I) and ammonia

Fuzhen Bi [a], Jun Gao [a,b,*], Lili Wang [a], Likai Du [a], Bo Song [c], Chengbu Liu [a,b]

[a] Key Lab of Colloid and Interface Chemistry, Ministry of Education, Institute of Theoretical Chemistry, School of Chemistry & Chemical Engineering, Shandong University, Jinan 250100, PR China
[b] Key Laboratory of Theoretical and Computational Chemistry in Universities of Shandong, Shandong University, Jinan 250100, PR China
[c] Shanghai Institute of Applied Physics, Chinese Academy of Sciences, Laboratory of Physical Biology, Shanghai 201800, PR China

ARTICLE INFO

Article history:
Received 4 July 2013
In final form 21 September 2013
Available online 30 September 2013

Keywords:
Halogen bond
σ-Hole
DFT-SAPT
Polarization
Electrostatic interaction
Charge transfer

ABSTRACT

Polarization plays an important role in halogen bond formation process. In this work, we proposed a polarization-enhanced bonding process of halogen bonds. Firstly, the energy differences between electrostatic interaction and point charge model are linearly correlated with polarization effects in studied dimers. The contribution of polarization to electrostatic interaction was 23.9% for the hydrogen bonded dimers, while it varied from 2.5 to 50.5% for the halogen bonded dimers. Secondly, we observed that the dominant term of polarization effects is different for hydrogen bonds, weak halogen bonds, and strong halogen bonds. In this study the dominant terms in the bonds change from the dispersion component to induction component gradually. Finally, we found that polarization and charge transfers are cooperated mutually. We feel these findings will be beneficial to designing better halogen bonded materials and lead to the development of polarizable force fields of halogen bonds.

1. Introduction

The halogen bond (XB), which is analogous to hydrogen bond (HB), has been studied via various experimental and theoretical methods recently [1–3]. The halogen bond is often described as R–X···B(X = Cl Br or I, B = N O S Se F^- Cl^- Br^- and I^-). Generally, the formation of halogen bonds involves the interaction of positive σ-holes (the positive region of electrostatic potential on the extensions of the covalent bond to the halogen) in the halogen with the Lewis base molecules [4,5]. At the same time, the existence of σ-hole makes the bond angle of XB fall into a very narrow range (approximately 180°) [5]. It is this highly directional property which may provide XB broad applications in molecular recognition [6–9], crystal engineering [7,10–12], super molecular chemistry [12–14] and biological systems [15,16].

In order to understand the halogen bond involved interactions, many experimental and theoretical works have been done. For example, Quantum mechanisms (QM) [3], Molecular mechanisms (MM) [17–20] and QM/MM methods have been used to theoretically study the properties of halogen bond involved systems [21,22]. These works indicate that the electrostatic effect, polarization, dispersion contributions, and the charge-transfer interactions are all important for the formation process of halogen bonds. Halogen bonds are closely related to the better-known hydrogen bonds as a result of both bonds having donor–acceptor distances that can be significantly shorter than the sum of their respective van der Waals radii [23]. Recently, Hennemann et al. introduced polarization-induced σ-hole in hydrogen bond systems [24]. The strong collinear polarizability of the A–H bond in A–H···B hydrogen bonds in his study is shown to lead to an enhanced σ-hole on the donor hydrogen atom and hence to a stronger hydrogen bonding. Also recently, several research groups have extended the existent force fields to halogen bonding systems based on the similarity of hydrogen and halogen bonds. Ibrahim developed the first force field for halogen bonding where the positive region centered on the halogen atom was represented by an extra point of charge (EP) [17,18]. Jorgensen et al. modified OPLS-AA Force Field to treatment halogen bonding, and tested an application to potent Anti-HIV agents [19]. Carter et al. derived a set of simple directional potential energy functions to model the shape and electrostatic properties of halogens, which, together, constitute a set of potential energy functions for a force field for biological halogen bonds (f f BXB) [23]. Our group also developed a polarizable ellipsoidal force field (PEff) for halogen bonds, in which the anisotropic charge distribution was represented with the combination of a negative charged sphere and a positively charged ellipsoid [25].

* Corresponding author at: Key Lab of Colloid and Interface Chemistry, Ministry of Education, Institute of Theoretical Chemistry, School of Chemistry & Chemical Engineering, Shandong University, Jinan 250100, PR China. Tel.: +86 531 88363967; fax: +86 531 88564464.
E-mail address: gaojun@sdu.edu.cn (J. Gao).

0301-0104/$ - see front matter © 2013 Elsevier B.V. All rights reserved.
http://dx.doi.org/10.1016/j.chemphys.2013.09.006

In our study we noticed that both the interaction energies span of halogen bonding and hydrogen bonding interactions are broader. The interaction energies of halogen bonds are 1–43 kcal/mol [6] and the hydrogen bonds are 0.2–40 kcal/mol. The broad transition regions merge continuously with the covalent bond, the van der Waals interaction and the halogen/hydrogen and the ionic or π interaction, and each type of the interactions has its own nature. The hydrogen bonds can be considered as incipient proton transfer reactions, seen from this perspective, the strong hydrogen bonds are in a very advanced state [26]. But how the halogen atoms can lead to such a broader halogen bond? We believe that exploring the origin forming progress of halogen bond can be beneficial to understanding halogen bonds essentially and the development of efficient force fields of halogen bonding interaction.

In order to answer these questions, we selected a series of halogen-bond complexes formed between F–X (X = F, Cl, Br, I) and ammonia as models; in addition, a hydrogen-bond complex formed between F–H and ammonia was also selected for comparison. The Symmetry Adapted Perturbation Theory (SAPT) was adopted for energy decomposition, which has been used to analyze the energy components in a variety of complexes, including hydrogen bond complexes [27,28], cation–π interactions [29], and halogen bond complexes [30]. Then, we defined the energy components as electrostatic interaction and non-electrostatic interactions terms. Comparing a systematic correlation analysis of these energy terms with point charge models, we addressed the relationship of halogen bonds and hydrogen bonds and found that the halogen bond adopts a polarization-enhanced bonding process.

2. Method

In order to perform high level quantum chemistry calculation, we selected a relatively small representational model system, the F–X (X = H, F, Cl, Br, I) and ammonia dimers. These dimers have been wildly adopted in studies of halogen bonds [31–33]. In this work we labeled the compounds as following: I, F–H$\cdots$NH$_3$; II, F–F$\cdots$NH$_3$; III, F–Cl$\cdots$NH$_3$; IV, F–Br$\cdots$NH$_3$; and V, F–I$\cdots$NH$_3$. The aug-cc-pVTZ basis set was used for geometric optimization of each dimer, except for iodine contained dimers, the iodine atom was described using the pseudopotential based aug-cc-pVTZ-PP basis set. The geometry of each dimer was optimized on the counterpoise (CP) corrected geometric hypersurface at the MP2 level [34]. This level of theory is adequate in order to provide reasonable results for weakly bonded interactions [35] and it was shown that the CP optimization method influences the geometry and the interaction energy with CP correction is much closer to the value at the CCSD(T)/aug-cc-pVQZ level [34], though the true basis set superposition error may be overestimated or underestimated a few [36,37]. The potential energy curves (PECs) for the five dimers were studied. Rigid monomer geometries were adopted because the frozen-monomer approximation worked reasonably well for PECs [38–40]. First, monomer geometries were obtained by MP2/aug-cc-pVTZ(aug-cc-pVTZ-PP on I) optimization. Then PECs were constructed with various halogen bond lengths starting from the equilibrium bond length and then continuously altered in incremental steps until they approximated the sum of van der Waals radii of halogen/hydrogen atom and nitrogen atom. The electronic wave function of F–Br$\cdots$NH$_3$ have been optimized at the CCSD(T) level for plotting the density difference. All these calculations were performed in GAUSSIAN 09 program [36].

Furthermore, the Multiwfn program [41,42] was used to analyze the topological properties of the complexes. The RESP program (version 2.2, available at http://q4md-forcefieldtools.org/RED/resp/) [43] was used to fit the Restrained Electrostatic Potential (RESP) charges of extra-point.

To discern the relative contribution of the interaction energy components, the energy decomposition analysis was calculated using the density functional theory combined with the symmetry adapted perturbation theory (DFT-SAPT) using MOLPRO2010.1 programs [39]. This method promised to yield results that agree remarkably well with SAPT method but with a much smaller computational cost [30]. The asymptotically corrected PBE0 (PBE0AC) exchange–correlation function and aug-cc-pVTZ (aug-cc-pVTZ-PP on I) basis set were both used in the DFT-SAPT approach, which is known to yield a reliable energy component [44–46]. The experimental ionization potentials were used for NH_3 [47], HF [48], F_2 [49], ClF [50], BrF [51], IF [51] within the asymptotic correction.

The motivation of this work is to find a feasible improvement protocol of current force fields of halogen bond. Generally, the electrostatic interactions are represented as fixed point charges in the force fields, where the total interaction energy of DFT-SAPT approachcan be defined as

$$E_{\text{int}} = E_{elst} + E_{exch} + E_{ind} + E_{disp} + \delta HF \tag{1}$$

These quantities refer to the electrostatic, exchange, induction and dispersion contributions to the overall interaction energies respectively. The δHF term is a Hartree–Fock correction term interpreted as the effects of third and higher order induction and exchange-induction effects which are not included within the other terms. Although there is no rigorous basis for defining such contributions not independent of each other, it is certain that the overall interaction energy is a physical observance [52], and the electrostatic interaction can be estimated [53] in DFT-SAPT theory. So, we rewrote the DFT-SAPT total interaction energy as following:

$$E_{\text{int}} = E_{elst} + E_{exch} + E_{nonelec} \tag{2}$$

$$E_{nonelec} = E_{ind} + E_{disp} + \delta HF \tag{3}$$

At the same time, the electrostatic interaction energy of two fixed point charges can be written as:

$$E^{P}_{elst} = C\frac{q_1 q_2}{R_{1,2}} \tag{4}$$

where C is a constant, q_1 and q_2 are amount of charges, $R_{1,2}$ is the distance of two charges. Considering that q_1 and q_2 are fixed in the force field, we may also write them as a constant:

$$E^{P}_{elst} = \frac{C'}{R_{1,2}} \tag{5}$$

It should be noted that E^{P}_{elst} should be a linear term of $\frac{1}{R_{1,2}}$. In the case of halogen bond formation procedure, several points along long bond lengths can be used to fit the parameter C′. The difference between E^{P}_{elst} and E_{elst} should also indicate the relative polarization effect with respects to the case that the halogen bond lengths is larger than the sum of van der Waals radii. It should be noted that the ΔE value is related to the some parts of the polarization but not all.

$$\Delta E = E^{P}_{elst} - E_{elst} \tag{6}$$

It is evident that the CT energy term is missing in the SAPT decomposition. Because the monomer energy is determined with dimer basis sets within DFT-SAPT, the default in MOLPRO calculations, the CT energy is partially covered in the second-order induction and mainly in the nonperturbative δHF term [54]. The CT energy can be approximated by the $E^{(2)}$ perturbation second-order energy evaluated within the nonbonding orbital (NBO) analysis [55]. Therefore, we performed NBO analyses for all of the dimers at the HF/aug-cc-pVTZ (aug-cc-pVTZ-PP on I) level. The CT can be calculated by [55]:

$$E^{(2)} = \frac{-2F_{\sigma\sigma^*}}{\varepsilon_{\sigma^*} - \varepsilon_{\sigma}} \tag{7}$$

$F_{\sigma\sigma}$ is the Fock matrix element between the i and j NBO orbital, ε_σ, ε_σ are the energies of σ^* and σ .

In order to explore the role of charge transfer in halogen bond, we make a series of correlation analyses between the CT energy and E_{elst}, ΔE, $E_{nonelec}$, E_{exch} and $E_{nonexch}$. Furthermore we defined the total affinity interaction $E_{nonexch}$ and showed the regulation of charge transfers to the total interaction energy explicitly.

$$E_{nonexch} = E_{\text{int}} - E_{exch} = E_{elst} + E_{nonelec} \tag{8}$$

3. Results and discussion

3.1. The polarization induced bonding process of halogen bond

The geometric parameters for optimized equilibrium structure of the dimers were shown in Table 1. For each dimer, 15 spots (10 spots for II) of halogen bond lengths were manually selected. A series of DFT-SAPT interaction energy decompositions were calculated and the interaction energy was shown in Support Information Table S1 and Tables S2–S11. Fig. 1 plots the dimers' curves of E_{elst} versus the reciprocal of halogen bond length (1/d(X–N)). The interaction energy curves descend rapidly and speed up with the shortening of each bond length. But, as described in Eq. (5), the E_{elst} should be the linear term of $1/R_{1,2}$ without considering the polarization occurring outside of van der Waals radius. So, the first six points (four points for II which have a larger equilibrium bond length relative to the sum of van der Waals radii) with the longer bond lengths were selected to fit a straight line as shown in Fig. 1(A). Such a selection is a bit underdeveloped, mainly because we chose to only focus on the relative polarization around equilibrium bond length. Considering that the points used to fit the line also have polarization effects, it is understandable that the lines do not cross the zero point. The correlation coefficients values of dimer I to V are 0.9947, 1.000, 0.9798, 0.9812, 0.9820, respectively, which shows that I and II dimers are slightly different from halogen bonded dimers III–V. The dimers I and II are hydrogen bonded and weak halogen bonded and the dimers III–V are bonded with strong and medium halogen bonds. Furthermore, the curves of E_{elst} will depart the fitted lines with the shortening of bond length. We assume that these differences should relate to the polarization effect which intend the charge density fluctuation from the free state, outside of van der Waals radius, to the form of halogen bond. So, the energy differences are calculated according to Eq. (6), and correlated to $E_{nonelec}$ terms of Eq. (3).

The correlations of the ΔE with the $E_{nonelec}$ and the corresponding fitting lines are show in Fig. 1(B). The correlation coefficients values of I to V are 0.9987, 0.9866, 0.9981, 0.9953, 0.9773, respectively. The absolute slope values of I to V are 0.4811, 0.7123, 0.8764, 0.9992 and 1.595 respectively. It indicates that the ΔE of halogen bond dimers (II–V) are strong cooperated with $E_{nonelec}$. The sequence II < III < IV < V also corresponds to the strength of halogen bond. It makes sense that the radii increases and the electronegativity decreases in the sequence of F, Cl, Br and I. This in turn makes the atoms become softer and softer and thus the atom's electron cloud density more susceptible to the electric field of ammonia. We also calculated the percentage of ΔE to E_{elst} at equilibrium bond length for each dimers (Table 2). Interestingly, the percentage of the hydrogen bond dimer is only 23.9%, agreeing with the reports of Hennemann et al. The polarization should result in an approximately 20% increase in hydrogen-bond strength [24], however the percentages hovered 44.7–50.5% in halogen-bond strength, except 2.48% for the weak halogen bonds with F as the donor. We concluded that the formation of halogen bonds are more so influenced by polarization effects than by hydrogen bonds. The polarization effects became stronger with the shortening of bond lengths because it is a polarization induced bonding process not a hydrogen one.

In order to further understand the bonding process of the halogen bond, we selected $FBr\cdots NH_3$ as the sample to plot the density shift before and after the formation of halogen bond. As shown in Fig. 2(a), a decrease of electron density occurred on the right side of

Table 1
Geometric parameters (Å and deg) for the optimized structure of the researched dimers in this work.

	d(X···N)	θ(F–X···N)	θ(X···N–H)
$FH\cdots NH_3$	1.696	179.34	111.62
$FF\cdots NH_3$	2.646	179.90	111.96
$FCl\cdots NH_3$	2.260[a]	179.98	110.21
$FBr\cdots NH_3$	2.327[a]	179.93	110.35
$FI\cdots NH_3$	2.481	179.99	110.78

[a] Dimers have been reported in a previous study (Ref. [34]).

Table 2
The percentages of ΔE to E_{elst} at equilibrium bond lengths for each dimers.

Dimer	$E_{nonelec}$	E_{elst} (kcal/mol)	ΔE (kcal/mol)	$\lvert\frac{\Delta E}{E_{elst}}\rvert$ (%)
I	−14.335	−21.139	5.0482	23.9
II	−3.0908	−3.4546	0.085702	2.48
III	−31.294	−35.813	18.085	50.5
IV	−33.790	−42.310	21.319	50.4
V	−27.049	−43.330	19.358	44.7

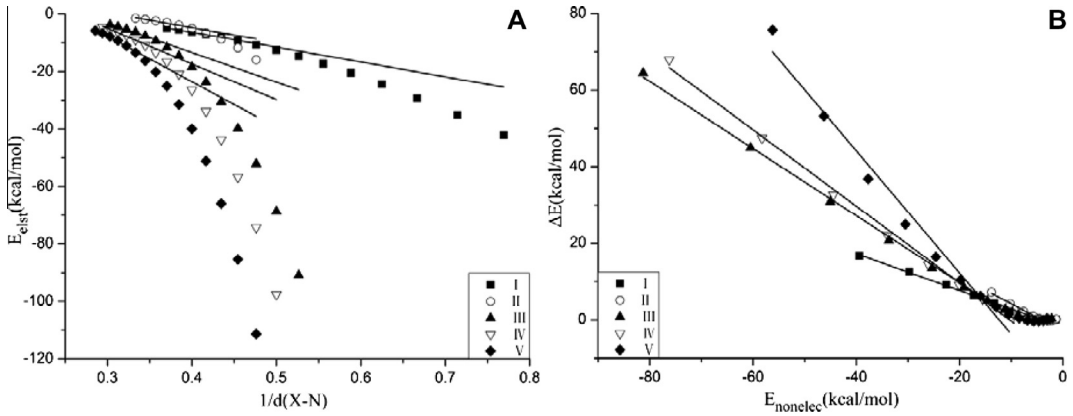

Fig. 1. (A) Plots of the electrostatic energy of halogen bonded and hydrogen bonded complexes versus the 1/d(X–N) and the resulting fitting line based on the selected points. (B) Correlation of the ΔE with the $E_{nonelec}$ and the fitting line (we select the closest nine (six for II)separation at which the polarization of halogen atom is the most obvious).

Br and oriented the halogen bond acceptor, while an increase of electron density occurred on the other side of bromine atom [56]. In addition, the increase also formed in the dumbbell-liked region of fluorine atoms along the direction of F–Br covalent bond. The decrease of the F–Br internuclear region agreed with the red shift of the corresponding frequency [34]. Such a pattern of electron density shifts are consistent with mutual polarization [57]. At the same time, a point charge model [24] was selected to mimic the polarization induced bonding process of halogen bonds. As shown in Fig. 2(b), when the point charge accesses the halogen atom, the change of σ-hole is facilely observed and characterized by the $V_{s,max}$ and the MEP. The size and strength increase of the σ-hole can be seen clearly, which indicates that the external electric field can induce more pronounced σ-holes.

The rising question now is about the performance of existent force fields in describing a polarization induced bonding process. In an previous experiment, Cieplak and Dixon have introduced an EP into the force field to mimic the lone pair of electrons on a Lewis base, and thus improving the electrostatic-potential and recovering hydrogen bond directionality [58,59]. The change of σ-holes could not be directly observed in the halogen bond complexes. So, an EP was adapted and then RESP charges of EP were fitted. Fig. 3 show that RESP charge increased as ammonia neared halogen atoms which reflects the fact that the ammonia induced more pronounced σ-holes. The RESP charges increased from 0 to 0.6e with the formation of the bonds. The amount of the increased values contributed to 50% or more of the RESP charges of equilibrium bond length which indicates that the polarization effects are important for halogen bonds. It also indicates that the parameters used for the EP of charge [18] may need reassignment when describing the bonding and breaking process of the halogen bond. We believe further proper development of halogen bond force fields are still in needed.

3.2. Analysis the contribution of polarization from hydrogen bond to halogen bond

The dispersion component and induction component are two terms closely related to the polarization among the nonelectrostatic interaction. The dispersion interaction concerns correlations between electron density fluctuations. It refers to the attractive interaction between the induced dipole and the temporary dipole. In general, the dispersion comes from the polarization and the polarization comes from the electrostatic interaction. Riley points out that polarization is an intrinsic part of the electrostatic interaction [60] and dispersion is a function of polarizability [36,61]. Both

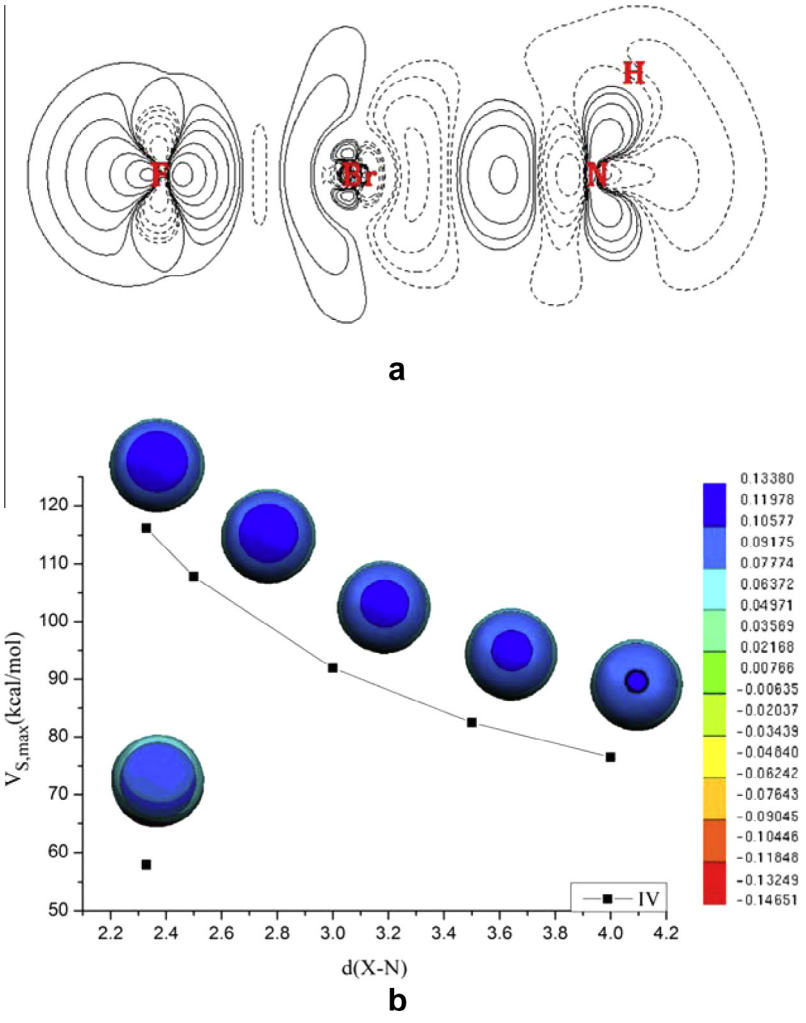

Fig. 2. (a) computed density difference plot for the FBr···NH_3 complexes. The solid lines represent the increases of the charge density, and the dashed lines represent the decreases of density. (b) Molecular electrostatic potential (MEP) maps of FBr mapped on the surfaces of molecular electron density and the maximum (positive) value of the MEP at the position of the σ-holes (electron density used to define molecular surface: 0.001 au). The top five point represent that there is a point charge of magnitude −0.878 at a distance of 2.33 Å, 2.500 Å, 3.000 Å, 3.500 Å and 4.000 Å respectively along the F–Br axis and the bottom point represent the case without a point charge.

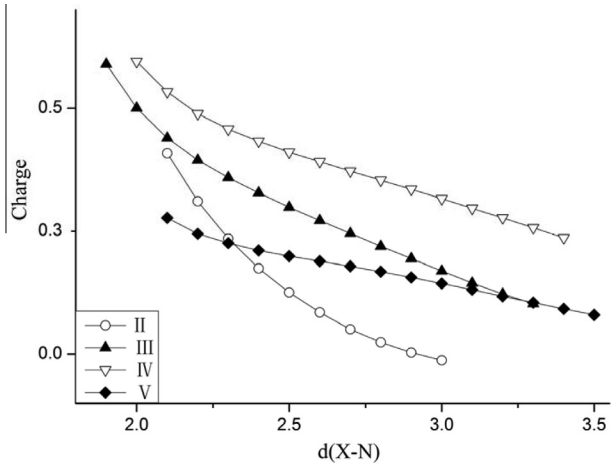

Fig. 3. Dependence between RESP charge and the halogen–nitrogen separation distance d(X–N) in Å. (the RESP charge was fitted in the situation where the separation of halogen atoms involved in halogen bond processing and extra-point (EP) was fixed at 1.5 Å.

the induction component and the dispersion component are second order effect, because they all originate from electron density distortion [62]. In Fig. 4, we present the relationship between these components and d(X–N) (it was shown in Support Information Fig. S1 for II). According to the DFT-SAPT calculation, the electrostatic contribution is dominant for I, II, III, IV and also for V when the d(X–N) is relatively larger. Interestingly, the domination came to be the induction contribution when the points near the potential energy minimum of the V complex. One of the most prominent features of these data is the fact that the induction contribution increased rapidly as the d(X–N) decreases. It increased −19.25, −0.8611, −64.39, −86.78, −218.3 kcal/mol corresponding to the change of the d(X–N) for the complex of I, II, III, IV and V respectively. The order of increase corresponds to the polarizability of halogen atoms involved in halogen bonds which is F < Cl < Br < I. The trend of the dispersion contribution is similar to the induction contribution but is more moderate [60]. The induction contribution is less than or equal to dispersion contribution when the ammonia is distant from halogen atom, but the induction increases rapidly and exceeds the dispersion contribution after the ammonia approaches the atom gradually, which becomes more obvious as the strength of halogen bond increases. It can be seen that the E_{ind} is larger than E_{disp} when the ammonia is the halogen bond acceptor. The increase of electrostatic component is very obvious for both the hydrogen bond and the halogen bond.

In fact, the concept of σ-hole bonding indicates that the halogen bond is an electrostatically-driven highly directional noncovalent interaction [63]. In a recent study, Hobza and Riley investigated the nature of X···OCH_2 halogen bonding employing symmetry adapted perturbation theory (SAPT) analyses and found that the largest SAPT interaction energy component for unfluorinated systems containing chlorine and bromine is dispersion, while for the iodomethane-formaldehyde complex is electrostatic interaction [30]. This means that the electrostatic composition increased rapidly followed by the increased size of halogen atoms, which is consistent with the change of the polarizability of halogen atoms.

It is also remarkable that not only the halogen atoms is involved in contributing to the polarization effect, but the halogen acceptor also plays an important role. Ban et al. have shown that the E_{ind} increases more rapidly than E_{disp} in order of $H_2CO\cdots ClF < H_2CS\cdots ClF < H_2CSe\cdots ClF$ [64], consistent with the polarizability of atoms. As for hydrogen bonds the E_{ind} is decreased and the E_{disp} is increased and both of the changes are far less than that of the halogen bond.

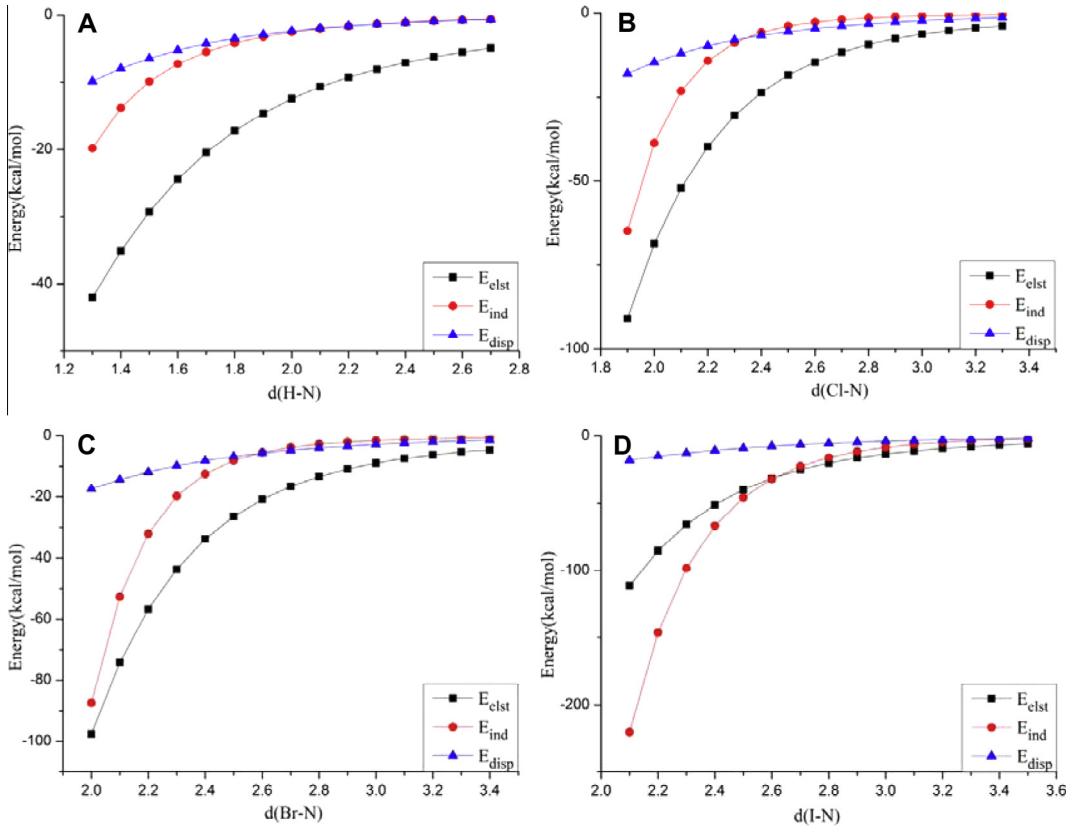

Fig. 4. Shows the electrostatic, induction, and dispersion component, for I, III IV and V for different variables of the halogen-nitrogen separation distance d(X–N) in Å.

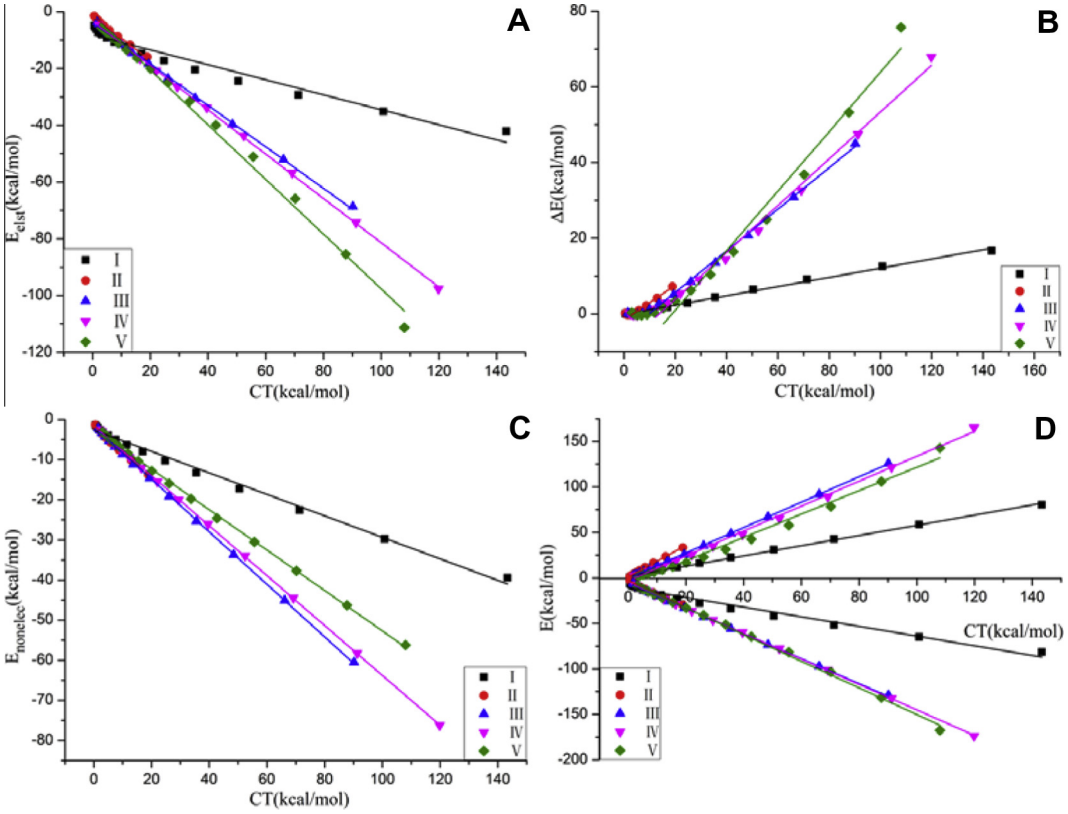

Fig. 5. The correlation analyses between CT energy and E_{elst} (A), ΔE (B), and $E_{nonelec}$ (C), respectively in I, II, III, IV and V dimer, and the relationship of E_{exch}, $E_{nonexch}$ and CT energy (D).

3.3. Cooperation of polarization and charge transfer

The formation of halogen bonds and hydrogen bonds are both strongly related to the donor–acceptor natural bond orbital interaction [55,65], but its contribution to the overall binding energy of hydrogen bonding and halogen bonding complex is still controversial [66]. Khaliullin et al. recently pointed out that the NBO method severely overestimates CT due to the non-variational treatment of the reference "zero CT" electronic state [66–68]. The perturbation $E^{(2)}$ energy can not be compared with the energy terms coming from DFT-SAPT perturbation theory. It only can be compared within different CT complexes and in turn provide information on the relative importance of the CT energy term. Since the aim of this section is to explore the variation trend during the formation of halogen and hydrogen bonds, the results of NBO analysis were acceptable enough to correlate with the DFT-SAPT energy terms.

In order to explore the relationship between the CT energy and E_{elst}, ΔE, $E_{nonelec}$, E_{exch} and $E_{nonexch}$, a series of correlation analyses were done as shown in Fig. 5. These results suggest that the E_{elst} is linearly associated with the CT energy and the correlation coefficients values are 0.9544, 0.9944, 0.9987, 0.9998, 0.9937 for I to V dimer respectively. As for the relationship between the CT and ΔE, the nine (six for II) points with shorter bond lengths were selected to fit a straight line as shown in Fig. 5(B) and the correlation coefficient values is 0.9933, 0.9946, 0.9977, 0.9942, 0.9797 for I to V dimer respectively. Chen and Martínez have discussed that charge transfer is an extreme manifestation of polarization [69], but at what distance does the "shifting" (polarization) of electronic charge become the "transfer" of electronic charge is not clear. Weinhold et al. has also have pointed out that, as monomer separation varies, the charge distributions can readjust in response to their mutual polarizing effects [55]. The CT energy and $E_{nonelec}$ is also linearly associated as shown in the following correlation coefficient values of 0.9924, 0.9937, 0.9996, 0.9999 and 0.9992 for the to V dimers respectively. Both ΔE and $E_{nonelec}$ represent the level of polarization of halogen atom as shown in Eqs. (3) and (6). So, it is better to say that the CT and the polarization has changed in a cooperative manner. However, CT certainly increases the electron density of the adjacent areas of halogen atoms, and looks as if it will offset the further polarization of halogen atoms, but in turn they reinforce each other as shown in Fig. 5(B) and (C). Not only does the polarization of halogen atoms result in the difference between halogen atoms and point charges, but CT also leads to the change of electron density around the halogen atom. The E_{exch} increase followed the increase of the CT energy during the formation of halogen bonds, and the $E_{nonexch}$ also increased as the result of the halogen donor and acceptor moving closer to each other. The role of E_{elst}, $E_{nonelec}$ and E_{exch} are different, and the halogen bonds interaction energy is codetermined by E_{exch} and $E_{nonexch}$ with the regulation of CT as shown in Fig. 5(D). So, we have concluded that the polarization and charge transfers are cooperated mutually and the interplay of exchange and charge transfer determines the bonding energy of halogen bonds. We are now on the way to further understanding how the interplay of exchange and charge transfer determines the bonding energy of halogen bonds and how it is associated with the softness and hardness of halogen bond formers, as Balazs Pinter et al. [70] explained in previous studies.

4. Conclusion

The halogen atoms will polarize when the ammonia, similar to the point charge, nears the halogen atom gradually. The polarization is the result of the distortion of electric density under the influence of the electric field of halogen acceptor and plays an

important role in the formation and strengthening of halogen bonds. CT can also regulate the strength of halogen bonds by causing the change of electric density around halogen bond donors and acceptors. In conclusion, the polarization and charge transfers, which are closely related to the softness and hardness of halogen donors and acceptors, are cooperated and the interplay of exchange and charge transfer codetermine the bonding energy of halogen bonds. Considering the softness and hardness of halogen donors and acceptor, we can try to choose the suited halogen atom and halogen bond acceptor to fine tune the strength of halogen bonds in biological system, materials chemistry, and so on.

Acknowledgments

This work is supported by the National Natural Science Foundation of China (Nos. 91127014 and 21373124), Doctoral Fund of Ministry of Education of China (No. 20110131120010), Natural Science Foundation of Shandong Province of China (No. ZR2010BZ005). It is also supported by Virtual Laboratory for Computational Chemistry, Supercomputing Center of Chinese Academy of Science and Shandong University High Performance Computing Center.

Appendix A. Supplementary data

Supplementary data associated with this article can be found, in the online version, at http://dx.doi.org/10.1016/j.chemphys.2013.09.006.

References

[1] A.R. Voth, P. Khuu, K. Oishi, P.S. Ho, Nat Chem 1 (2009) 74–79.
[2] S.M. Walter, F. Kniep, L. Rout, F.P. Schmidtchen, E. Herdtweck, S.M. Huber, J Am Chem Soc 134 (2012) 8507–8512.
[3] A.J. Parker, J. Stewart, K.J. Donald, C.A. Parish, J Am Chem Soc 134 (2012) 5165–5172.
[4] P. Politzer, P. Lane, M. Concha, Y. Ma, J. Murray, J Mol Model 13 (2007) 305–311.
[5] T. Clark, M. Hennemann, J. Murray, P. Politzer, J Mol Model 13 (2007) 291–296.
[6] P. Metrangolo, H. Neukirch, T. Pilati, G. Resnati, Accounts Chem Res 38 (2005) 386–395.
[7] C.B. Aakeröy, M. Fasulo, N. Schultheiss, J. Desper, C. Moore, J Am Chem Soc 129 (2007) 13772–13773.
[8] E. Corradi, S.V. Meille, M.T. Messina, P. Metrangolo, G. Resnati, Tetrahedron Lett 40 (1999) 7519–7523.
[9] D.B. Fox, R. Liantonio, P. Metrangolo, T. Pilati, G. Resnati, J Fluorine Chem 125 (2004) 271–281.
[10] D. Cinčić, T. Friščić, W. Jones, Chem Eur J 14 (2008) 747–753.
[11] D. Cincíci, T. Friscíc, W. Jones, in: J Am Chem Soc 130 (2008) 7524–7525.
[12] P. Metrangolo, F. Meyer, T. Pilati, G. Resnati, G. Terraneo, Angew Chem Int Ed 47 (2008) 6114–6127.
[13] S. Derossi, L. Brammer, C.A. Hunter, M.D. Ward, Inorg Chem 48 (2009) 1666–1677.
[14] T. Shirman, T. Arad, M.E. van der Boom, Angew Chem Int Ed 49 (2010) 926–929.
[15] A.R. Voth, F.A. Hays, P.S. Ho, Proc Natl Acad Sci USA 104 (2007) 6188–6193.
[16] P. Auffinger, F.A. Hays, E. Westhof, P.S. Ho, Proc Natl Acad Sci USA 101 (2004) 16789–16794.
[17] Ibrahim, A.A. Mahmoud, J Phys Chem B 116 (2012) 3659–3669.
[18] Ibrahim, A.A. Mahmoud, J Comput Chem 32 (2011) 2564–2574.
[19] W.L. Jorgensen, P. Schyman, J Chem Theory Comput 8 (2012) 3895–3901.
[20] Ibrahim, A.A. Mahmoud, J Mol Model 18 (2012) 4625–4638.
[21] Y. Lu, T. Shi, Y. Wang, H. Yang, X. Yan, X. Luo, H. Jiang, W. Zhu, J Med Chem 52 (2009) 2854–2862.
[22] Ibrahim, A.A. Mahmoud, J Chem Inf Model 51 (2011) 2549–2559.
[23] M. Carter, A.K. Rappé, P.S. Ho, J Chem Theory Comput 8 (2012) 2461–2473.
[24] M. Hennemann, J. Murray, P. Politzer, K. Riley, T. Clark, J Mol Model 18 (2012) 2461–2469.
[25] L. Du, J. Gao, F. Bi, L. Wang, C. Liu, J Comput Chem 34 (2013) 2032–2040.
[26] T. Steiner, Angew Chem Int Ed 41 (2002) 48–76.
[27] A. Fiethen, G. Jansen, A. Hesselmann, M. Schütz, J Am Chem Soc 130 (2008) 1802–1803.
[28] H. Szatyłowicz, T.M. Krygowski, J.J. Panek, A. Jezierska, J Phys Chem A 112 (2008) 9895–9905.
[29] I. Soteras, M. Orozco, F.J. Luque, Phys Chem Chem Phys 10 (2008) 2616–2624.
[30] K.E. Riley, P. Hobza, J Chem Theory Comput 4 (2008) 232–242.
[31] J.W. Zou, Y.J. Jiang, M. Guo, G.X. Hu, B. Zhang, H.C. Liu, Q.S. Yu, Chem Eur J 11 (2005) 740–751.
[32] Q.Z. Li, Q.Q. Lin, W.Z. Li, J.B. Cheng, B.A. Gong, J.Z. Sun, Chemphyschem 9 (2008) 2265–2269.
[33] J.Y. Wu, J.C. Zhang, Z.X. Wang, W.L. Cao, J Chem Theory Comput 3 (2006) 95–102.
[34] P.P. Zhou, W.Y. Qiu, S. Liu, N.Z. Jin, Phys Chem Chem Phys 13 (2011) 7408–7418.
[35] K.E. Riley, P. Hobza, J Phys Chem A 111 (2007) 8257–8263.
[36] G. Chałasiński, M.M. Szczęśniak, Chem Rev 100 (2000) 4227–4252.
[37] E.R. Davidson, D. Feller, Chem Rev 86 (1986) 681–696.
[38] K.U. Lao, J.M. Herbert, J Phys Chem A 116 (2012) 3042–3047.
[39] R. Podeszwa, R. Bukowski, K. Szalewicz, J Phys Chem A 110 (2006) 10345–10354.
[40] R. Podeszwa, R. Bukowski, B.M. Rice, K. Szalewicz, Phys Chem Chem Phys 9 (2007) 5561–5569.
[41] T. Lu, Multiwfn, Version 2.4 http://multiwfn.codeplex.com.
[42] T. Lu, F. Chen, J Comput Chem 33 (2012) 580–592.
[43] C.I. Bayly, P. Cieplak, W. Cornell, P.A. Kollman, J Phys Chem 97 (1993) 10269–10280.
[44] A. Heßelmann, G. Jansen, Phys Chem Chem Phys 5 (2003) 5010–5014.
[45] A. Heßelmann, G. Jansen, Chem Phys Lett 367 (2003) 778–784.
[46] H.L. Williams, C.F. Chabalowski, J Phys Chem A 105 (2000) 646–659.
[47] F. Qi, L.S. Sheng, Y.W. Zhang, S.Q. Yu, W.-K. Li, Chem Phys Lett 234 (1995) 450–454.
[48] G. Bieri, A. Schmelzer, L. Åsbrink, M. Jonsson, Chem Phys 49 (1980) 213–224.
[49] H. Van Lonkhuyzen, C.A. De Lange, Chem Phys 89 (1984) 313–322.
[50] R.L. DeKock, B.R. Higginson, D.R. Lloyd, A. Breeze, D.W.J. Cruckshank, D.R. Armstrong, Mol Phys 24 (1972) 1059–1072.
[51] J.M. Dyke, G.D. Josland, J.G. Snijders, P.M. Boerrigter, Chem Phys 91 (1984) 419–424.
[52] P. Hobza, R. Zahradník, K. Müller-Dethlefs, Collect Czech Chem C 71 (2006) 443–531.
[53] B. Jeziorski, R. Moszynski, K. Szalewicz, Chem Rev 94 (1994) 1887–1930.
[54] A.J. Stone, A.J. Misquitta, Chem Phys Lett 473 (2009) 201–205.
[55] A.E. Reed, L.A. Curtiss, F. Weinhold, Chem Rev 88 (1988) 899–926.
[56] P. Politzer, J.S. Murray, Chemphyschem 14 (2013) 278–294.
[57] P. Politzer, K.E. Riley, F.A. Bulat, J.S. Murray, Comput Theor Chem 998 (2012) 2–8.
[58] P. Cieplak, J. Caldwell, P. Kollman, J Comput Chem 22 (2001) 1048–1057.
[59] R.W. Dixon, P.A. Kollman, J Comput Chem 18 (1997) 1632–1646.
[60] K. Riley, J. Murray, J. Fanfrlík, J. Řezáč, R. Solá, M. Concha, F. Ramos, P. Politzer, J. Mol. Model., 1–9, http://dx.doi.org/10.1007/s00894-012-1428-x.
[61] P. Hobza, R. Zahradník, Int J Quantum Chem 42 (1992) 581–590.
[62] Alagona G, Ghio C. Ab initio theoretical methods for studying intermolecular forces. In: Química Fd, (Ed.) Introduction to Advanced Topics of Computational Chemistry, 2003, pp. 137–147.
[63] P. Politzer, J.S. Murray, T. Clark, Phys Chem Chem Phys 12 (2010) 7748–7757.
[64] Q.F. Ban, R. Li, Q.Z. Li, W.Z. Li, J.B. Cheng, Comput Theor Chem 991 (2012) 88–92.
[65] M.I. Bernal-Uruchurtu, R. Hernández-Lamoneda, K.C. Janda, J Phys Chem A 113 (2009) 5496–5505.
[66] R.Z. Khaliullin, A.T. Bell, M. Head-Gordon, Chem Eur J 15 (2009) 851–855.
[67] E. Munusamy, R. Sedlak, P. Hobza, Chemphyschem 12 (2011) 3253–3261.
[68] S. Karthikeyan, R. Sedlak, P. Hobza, J Phys Chem A 115 (2011) 9422–9428.
[69] J. Chen, T.J. Martínez, Chem Phys Lett 438 (2007) 315–320.
[70] B. Pinter, N. Nagels, W.A. Herrebout, F. De Proft, Chem Eur J 19 (2013) 519–530.